ORIGINAL RESEARCH

Diffusion Tensor–MRI Evidence for Extra-Axonal Neuronal Degeneration in Caudate and Thalamic Nuclei of Patients with Multiple Sclerosis

S. Hannoun
F. Durand-Dubief
C. Confavreux
D. Ibarrola
N. Streichenberger
F. Cotton
C.R.G. Guttmann
D. Sappey-Marinier

BACKGROUND AND PURPOSE: MS is an inflammatory demyelinating disease affecting both WM and GM. While WM lesions are easily visualized by conventional MR imaging, the detection of GM alterations remains challenging. This diffusion tensor MR imaging study aimed to detect and characterize diffuse microscopic alterations in 2 deep GM structures, the caudate nucleus and the thalamus, in patients with RR and SP MS. The relationship between diffusivity markers, and atrophy of the caudate and the thalamus, as well as brain lesion load and clinical status of the patients was also explored.

MATERIALS AND METHODS: Twenty-three RR and 18 SP patients, along with 27 healthy controls, underwent MR imaging examination including anatomic and DTI acquisitions. Volumes, mean FA, and MD of the caudate and the thalamus, as well as WM lesion volumes, were assessed.

RESULTS: FA was significantly ($P < .001$) increased in the caudate and the thalamus of patients with MS compared with controls, and was higher in SP compared with RR patients. Increased FA was associated with volume decreases of caudate ($r = -0.712$; $P < .001$) and thalamus ($r = -0.407$; $P < .01$) in patients with MS. WM T2 lesion load was significantly associated with caudate ($r = 0.611$; $P < .001$) and thalamic ($r = 0.354$; $P < .05$) FA. Caudate FA, and, to a lesser extent, thalamic FA, were associated with functional deficits, as measured by EDSS and MSFC.

CONCLUSIONS: Increased FA in the caudate and the thalamus may constitute a sensitive marker of MS pathologic processes, such as loss of dendrites and/or swelling of neuronal cell bodies.

ABBREVIATIONS: DD = disease duration; EDSS = Expanded Disability Status Scale; FA = fractional anisotropy; FMRIB = Functional Magnetic Resonance Imaging of the Brain; GM = gray matter; ICV = intracranial volume; MD = mean diffusivity; MSFC = Multiple Sclerosis Functional Composite; PD = proton attenuation; RR = relapsing-remitting; SP = secondary-progressive; T2-LL = T2-lesion load

Although MS has traditionally been considered a WM disease, pathologic studies dating back to the 19th century,[1,2] along with more recent reports,[3,4] have identified GM involvement. However, in vivo detection of GM alterations by conventional clinical imaging techniques is still challenging due to both limited tissue contrast and spatial resolution. Diffuse microscopic alterations and GM tissue loss can, however, be quantified in subcortical GM structures by DTI and volumetric measurement, respectively.

Volumetric assessment has become a well-established method for the measurement of GM brain atrophy, which has been shown to progress more rapidly than either WM or whole-brain tissue loss[5,6] in several cortical regions as well as in subcortical GM structures.[7,8] Indeed, volume reduction of deep nuclei has been demonstrated at the earliest clinical stages of MS,[9-11] while cortical GM involvement was identified later in the disease course.[12]

Numerous studies have applied DTI to characterize microstructural damage in cerebral WM and have demonstrated abnormal low FA and high MD in patients with MS demonstrating a change in myelin architecture.[13,14] However, only a few studies have investigated the subcortical GM structures and have found, contrarily to WM, an increase of tissue anisotropy.[15,16] The exact mechanisms responsible for these alterations are yet to be explored, especially because these variations may result from several causes, being either methodologic or physiopathologic.

In the present study of patients with RR and SP MS, we used DTI to detect diffuse microscopic changes in the caudate nuclei and the thalamus, 2 GM structures with distinct microarchitectures, and GM/WM ratios (Fig 1). Our overarching working hypothesis was that DTI metrics allow detection and characterization of neurodegenerative changes of brain GM primarily affecting the neuronal cell bodies and their dendrites. To shed light on the relationship between gradual microstructural alterations within nuclei and the macroscopic reduction of their volume, we studied the relationship between DTI metrics and volume measurements of both the thalamus and the caudate. To evaluate the possible effect of WM disease on GM degeneration, we also described the relationship between DTI measurements and the volume of WM lesions. These DTI metrics were

Received July 27, 2011; accepted after revision November 10, 2011.

From CREATIS, UMR 5220 CNRS & U1044 INSERM (S.H., F.D.-D., F.C., D.S.-M.), Université Claude Bernard-Lyon1, University of Lyon, France; Service de Neurologie (F.D.-D., C.C.), Service de Neuropathologie (N.S.), and Service de Radiologie (F.C.), Hôpital Neurologique, Lyon, France; Département IRM–CERMEP-Imagerie du Vivant (D.I., D.S.-M.), Lyon, France; Center for Neurological Imaging, Partners Multiple Sclerosis Center, Departments of Neurology and Radiology (C.R.G.G.), Brigham and Women's Hospital, Harvard Medical School, Boston, Massachusetts.

This research was sponsored by the French government grant "PHRC 2004" and the Région Rhône-Alpes, and was also supported by a public grant from the French Agence Nationale de la Recherche within the context of the Investments for the Future program, referenced ANR-10-COHO-002.

Please address correspondence to Dominique Sappey-Marinier, CERMEP-Imagerie du Vivant, 59 Boulevard Pinel, 69677 Bron Cedex, France; e-mail: sappey-marinier@univ-lyon1.fr

Indicates open access to non-subscribers at www.ajnr.org

Indicates article with supplementary on-line tables.

http://dx.doi.org/10.3174/ajnr.A2983

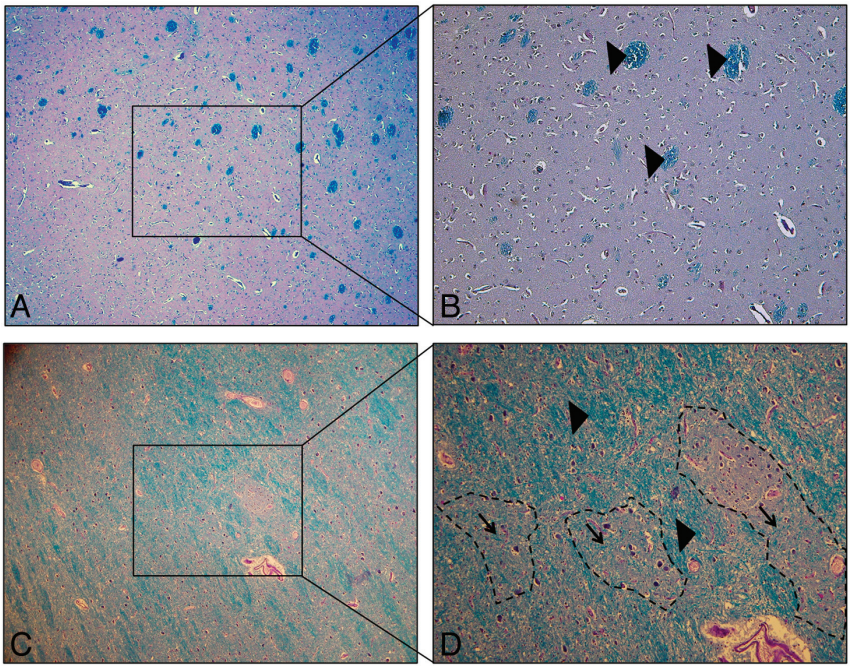

Fig 1. Microscopic views (Luxol fast blue-periodic-acid-Schiff) at 2 magnifications of 40X (*A–C*) and 100X (*B–D*) showing healthy GM, with a few scattered bundles of myelin (*blue*) in the caudate nucleus (*A* and *B*) and islets of GM surrounded by numerous myelin sheets (*blue*) in the thalamus (*C* and *D*) of a subject who was not part of this study and who died from a non-neurologic disorder. *B* shows well-delineated, sparsely distributed WM bundles (*large arrowheads*) within the homogeneous cytoarchitecture of the caudate nucleus. *D* shows that myelinated fiber bundles occupy a large fraction of the thalamic complex, both between (*large arrowheads*) as well as within (*small arrowheads*) thalamic subnuclei (shown with dotted outlining), where they are interspersed with neuronal cell bodies, providing the necessary intra- and extrathalamic connectivity. It is evident that myelinated WM fibers are much more prevalent in the thalamus compared with the caudate nucleus, providing a plausible explanation for the finding of higher peak FA in the thalamus of healthy controls compared with that of their caudate nuclei.

Table 1: Clinical characteristics and MRI lesion-load of MS patient subgroups

Patients	DD (years)	EDSS	MSFC	T2-LL (%)
RR (n = 23)	5.5 ± 2.6 (1.9–10.3)	2.4 ± 1.6 (0.0–4.5)	1.59 ± 1.10 (−0.83–3.38)	0.32 ± 0.26 (0.01–0.86)
SP (n = 18)	15.9 ± 4.3 (9.9–23.0)	5.4 ± 1.1 (4.0–7.0)	−1.25 ± 1.98 (−4.90–1.15)	0.64 ± 0.35 (0.11–1.31)

Note:—Values are reported as mean ± standard deviation (range).

then related with age, DD, and functional disability indices to evaluate the clinical impact of the measured deep GM alterations with regard to motor and cognitive functions.

Materials and Methods

Subjects

Forty-two patients with MS from a longitudinal MR imaging study and 29 control subjects were recruited. One patient with RR MS and 2 control subjects were excluded from the study due to the poor quality of their T1-weighted MR imaging, which made it impossible to obtain adequate image registration using FreeSurfer (http://surfer.nmr.mgh.harvard.edu). At initial enrollment, the remaining 41 patients had a diagnosis of definite MS according to the McDonald criteria[17] and an EDSS rating of 6 or lower. Because the presented DTI sequence was not included in the MR imaging protocol at study onset, some of the patients had more severe disability at the time of DTI measurement. All patients had a full neurologic history and neurologic examination performed by a board-qualified neurologist, including the EDSS and the MSFC. Twenty-three patients with RR (19 women and 4 men; mean age 33.8 ± 7.6 years), and 18 patients with SP (7 women and 11 men; mean age 41.7 ± 5.2 years) MS were studied, along with 27 healthy volunteers (15 women and 12 men; mean age 36.3 ± 8.7 years) with normal neurologic examination and no history of neurologic disorders (Table 1). Local ethical committee approval and written informed consent from all participants were obtained.

Image Acquisition

MR imaging acquisitions were performed on a 1.5T Sonata system (Siemens, Erlangen, Germany) with an 8-element phased-array head coil. The conventional MR imaging protocol included a 3D multiplanar reconstruction T1-weighted (TR = 1880 ms, TE = 4 ms, TI = 1100 ms) sequence, with and without gadolinium injection, yielding 176 sagittal 1-mm-thick sections. A TSE sequence was used to acquire 46 axial 3-mm-thick sections of PD and T2-weighted contrasts (TR = 3000 ms, TE = 12 ms, 85 ms). A FLAIR TSE sequence (TR = 8000 ms, TE = 105 ms, TI = 2200 ms) was also applied, with similar geometry (46 axial contiguous 3-mm-thick sections).

A 2D spin-echo multisection EPI DTI sequence (TE = 86 ms, TR = 6900 ms, acquisition time of 7 minutes) was used to acquire 51 axial sections parallel to the anterior/posterior commissure line, with 24 diffusion-gradient directions (b = 1000 seconds/mm^2) and a section thickness of 2.5 mm. A nominal isotropic 2.5 mm^3 resolution was obtained using a matrix size of 96 × 96 over a field of view of 240 × 240 mm. The B0 image was acquired 4 times to increase signal intensity–to-noise ratio.

Postprocessing and Image Analysis

Volume Analysis. Volumetric segmentation of the caudate nuclei and the thalamus was performed using the FreeSurfer v4.5 image analysis suite. The automated analysis of the 3D multiplanar reformation T1-weighted images included the following preprocessing procedures: motion correction, removal of nonbrain tissue using a hy-

Table 2: DTI metrics obtained with the direct outlining method and volume values

	Caudate			Thalamus		
	MD	FA	Volume	MD	FA	Volume
Controls	0.733 ± 0.029	0.195 ± 0.015	0.478 ± 0.053	0.719 ± 0.016	0.301 ± 0.014	0.984 ± 0.073
RR	0.751 ± 0.033	0.235 ± 0.027***	0.448 ± 0.054	0.732 ± 0.016*	0.325 ± 0.015***	0.893 ± 0.091**
SP	0.744 ± 0.022	0.270 ± 0.027***#	0.393 ± 0.062***†	0.736 ± 0.025**	0.341 ± 0.027***‡	0.833 ± 0.143***

Note:—Values are reported as mean ± standard deviation. Patients vs controls: * $P < .05$; ** $P < .01$; *** $P < .001$; RR vs SP: ‡ $P < .05$; † $P < .01$; # $P < .001$.

brid watershed/surface deformation procedure, and automated Talairach transformation. The segmentation[18,19] of deep GM structures was then followed by several postprocessing methods, including intensity normalization, tessellation of the GM/WM boundary, automated topology correction, and surface deformation of GM/WM and GM/CSF borders. Caudate and thalamus outlines were visually assessed and manually corrected, if necessary, and their volumes were normalized by the ICV to account for intersubject variability.

DTI Processing. Two approaches were applied to delineate the ROIs of the caudate and thalamus. First, a direct manual outlining was performed on the FA maps by an experienced observer, using MedINRIA software (http://www-sop.inria.fr/asclepios/software/MedINRIA/). Because the studied GM structures are poorly delineated from surrounding WM on FA maps, λ1 maps were used as guidance. In addition, to account for partial volume effects at the interface of GM and CSF, a systematic, 1-voxel erosion of the ROIs was applied at the edges of the ventricles. Because this approach might be perceived as biased, because the ROIs were outlined on the DTI images that were also used for the measurements of interest, a second approach was applied to validate our findings. The FreeSurfer-derived masks of the caudate and thalamic nuclei, segmented from the T1-weighted images, were coregistered and overlaid onto the FA and MD maps. To reduce partial volume effects at tissue boundaries with WM and CSF, the caudate and thalamus masks were first eroded by 1 layer of millimetric pixels. For the coregistration of segmented outlines, T1-weighted images were registered to the B0 images (DTI without diffusion weighting [$b = 0$ seconds/mm^2]), and the resulting affine transformation was applied to the caudate and thalamus masks using a nearest-neighbor interpolation. Visual assessment of the coregistered ROIs was performed by an experienced observer to validate the correctness of ROI position, and manual correction was performed as needed.

Analyses of diffusion tensor data were performed using the FMRIB Software Library.[20] First, eddy current correction, using the FMRIB Diffusion Toolbox, was applied, followed by a stripping of nonbrain voxels using the Brain Extraction Tool, with a fractional intensity threshold of 0.35.[21] Second, FA and MD maps were generated using the FMRIB Diffusion Toolbox module. MD and FA histograms within the caudate and thalamic nuclei were generated separately using the direct ROI outlining method and the FreeSurfer ROI overlay method for each subject. The peak position value was determined for FA and MD after fitting the histograms with a Gaussian function.

To assess methodologic noise in CSF, FA was measured in the frontal horns of the lateral ventricles in 5 randomly selected patients. A scan–rescan test was also performed to test the reproducibility of our measures on DTI acquisitions of the same control subject repeated over 10 consecutive days. The variation coefficients of the FA values obtained from the caudate and thalamus ROIs were calculated by dividing the standard deviation by the mean value.

Lesion Segmentation. T2-LL measurements were extracted from coregistered T1-, T2-, PD-weighted, and FLAIR images using an automatic segmentation algorithm in the SepINRIA (http://www-sop.inria.fr/asclepios/software/SepINRIA/) software.[22] The lesion masks were manually corrected and validated by an experienced neurologist before calculating the lesion volume. T2-lesion volume was then normalized by subject ICV.

Statistical Analyses

Statistical analyses of DTI and volumetric results were performed using data analysis and statistical software (STATA, version 9.2; StataCorp, College Station, Texas). The diffusivity parameters and the GM nuclei volumes measured in patients and controls were compared using a 1-way ANOVA test. Bonferroni correction was used to adjust for post hoc multiple comparisons. Correlation analysis was performed between the MR imaging–derived metrics (volumes, diffusion metrics, and lesion load) and age or clinical scores (DD, EDSS, and MSFC) using Spearman correlation. The significance threshold was set at $P < .05$.

Results

The results obtained from direct outlining and those obtained from the overlay of FreeSurfer-derived ROIs were similar but showed a few discrepancies. The latter provided results with larger standard deviations than the direct manual delineation, particularly in MD values. In addition, the FA values obtained by the direct manual outlining in the caudate and the thalamus were in better agreement with those reported in the literature.[15,16] For these reasons, we chose to detail the results obtained by the direct delineation method, and provide those obtained by the second method as supplementary data.

DTI measurements showed consistently higher FA in the thalamus compared with the caudate in all groups of subjects, reflecting the greater proportion of myelinated fibers in the thalamus (Table 2, On-line Table 1, Fig 2). FA values were significantly increased in both the caudate and thalamus of RR ($P < .001$) and SP patients ($P < .001$) compared with controls, and SP patients had significantly higher values than RR patients. Significant increases of MD were found in the thalamus of RR ($P < .05$) and SP patients ($P < .05$) compared with control subjects, whereas no differences were observed in the caudate (significance for this finding was reached only in the primary analysis but not in the secondary overlay analysis). Volumes of both structures were significantly decreased in SP patients compared with healthy controls. A decreasing trend for these measures was observed across the 3 groups of subjects (from controls to RR and SP patients) for both structures, but statistical significance between RR patients and controls was only attained for the thalamus, while only the caudate showed a significant decrease between RR and SP patients. Interestingly, FA values of the caudate were significantly higher in RR patients compared with controls, even though the caudate volumes were statistically indistinguishable between these 2 groups. FA increases were significantly correlated with the volume changes of both GM structures in pa-

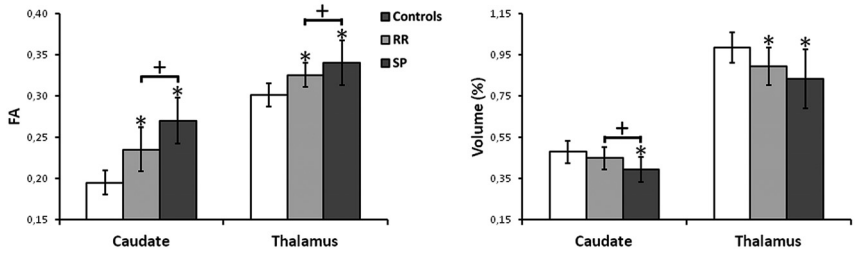

Fig 2. Histogram of FA and volume measures in the caudate and thalamus of patients with MS and control subjects (* indicates significant difference between patients and controls; +, significant difference between RR and SP MS patients).

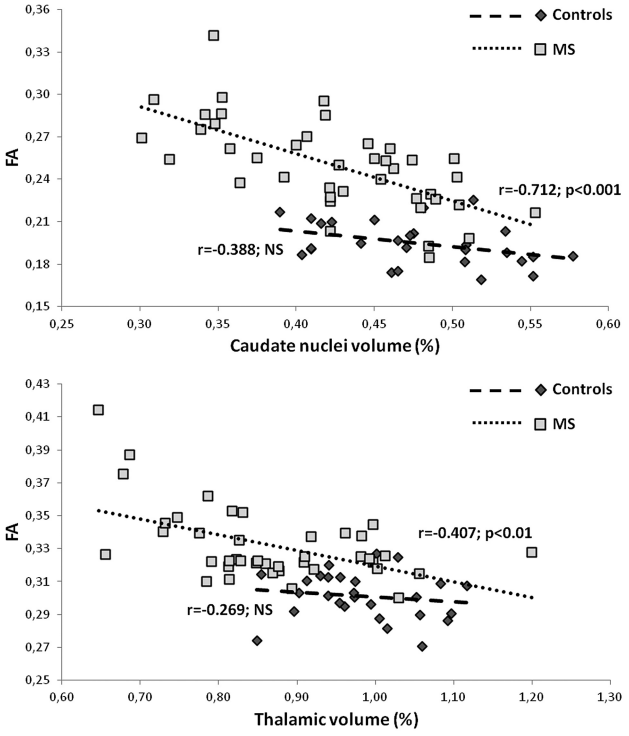

Fig 3. Correlation of FA and volume measures (*r* value) in both caudate and thalamus of MS patients (*dotted lines*) and control subjects (*dashed lines*).

tients with MS (caudate: $r = -0.712$, $P < .001$; thalamus: $r = -0.407$, $P < .01$), whereas this association was not found in healthy controls (Fig 3). The secondary overlay analysis also confirmed the FA-to-volume relationship in all patients with MS, including both RR and SP subgroups (On-line Table 2).

Taken together, these findings suggest that FA is sensitive to GM degeneration, and particularly so in the caudate. Table 3 and On-line Table 2 summarize the correlation statistics obtained between age, clinical scores (DD, EDSS, and MSFC), and MR imaging–derived metrics (lesion load, volumes, and DTI metrics) in the caudate and thalamus of all (RR+SP) patients with MS. FA and volume of the caudate and thalamus, but not their MD, were strongly associated with T2-LL. This relation was not confirmed for the caudate in the FreeSurfer-based overlay analysis, probably due to the inclusion in the ROIs of surrounding WM (MD increases were observed with both analytical approaches). In addition, FA values of the caudate were significantly correlated with DD. Finally, among all MR imaging metrics, the best predictor of EDSS or MSFC was the FA measurement in the caudate. The secondary analysis using FreeSurfer-derived overlays showed some notable differences compared with the primary analysis, but was nevertheless consistent with the main overall conclusions of this work (see On-line Table 2). We ascribe these differences to increased methodologic variability of the overlay method.

To characterize our method's sensitivity, we measured FA in the CSF of 5 subjects and found a mean (±SD) of 0.044 (±0.005), which corresponds to a potential bias of 16%–19% in the caudate and 12%–14% in the thalamus of RR and SP patients, respectively. In addition, our scan–rescan reproducibility test showed a FA variation coefficient of 2.64% in the thalamus and 4.65% in the caudate.

Discussion

The major findings of this study are the increased FA in both caudate and thalamic nuclei of patients with MS compared with healthy controls, the significant FA differences between RR and SP MS patient subgroups, and the relationship between caudate and thalamic FA and the extent of their atrophy and of clinical disease severity (EDSS and MSFC). The stronger relationship between FA and DD in the caudate compared with the thalamus suggests that this FA change is driven by damage to extra-axonal components of these structures.

Indeed, a healthy caudate nucleus presents a near-isotropic structure, mostly composed of neuronal cell bodies and dendritic connections, whereas the thalamus is composed of subnuclei that are separated by highly anisotropic myelinated fibers, as shown in Fig 1. This difference in tissue composition between the caudate and the thalamus was reflected by the FA difference between these structures in healthy controls as shown in Fig 4. Thus, we speculate that the marked increase of FA in the caudate is due to alterations of the neuronal cell micro-organization, and suggests, more specifically, that this increase might be attributed primarily to the loss of dendritic connections.[23]

Histopathologic studies of experimental animal models have shown neuritic beading and/or synaptic stripping, which have been tentatively ascribed to excitotoxicity[24] and the effect of activated microglia.[25] Cell culture studies have also reported interferon-gamma interference that selectively induces retraction of existing dendrites, ultimately leading to an 88% decrease in the arbor size.[26] Further, the relation between FA value and dendritic attenuation has been evidenced during early human brain development. At gestational age, GM cytoarchitecture is dominated by radial glial fibers of the cortical strata and apical dendrites of pyramidal cells, leading to nonzero anisotropy values. With time, this architecture is disrupted by the addition of basal dendrites as well as thalamocortical afferents, which progressively tend to reduce the

Table 3: Correlation coefficients between DTI metrics, obtained with the direct outlining method, other MRI metrics, and clinical scores in all patients with MS

	Age	DD	EDSS	MSFC	T2-LL	Volume
Caudate						
T2-LL	0.230	0.413**	0.250	−0.256	–	–
MD	−0.180	0.028	−0.247	0.413*	−0.094	0.150
FA	0.346*	0.417**	0.444**	−0.495**	0.611***	−0.712***
Volume	−0.373*	−0.315*	−0.223	0.366*	−0.481**	–
Thalamus						
MD	−0.247	−0.039	0.043	0.176	0.014	0.100
FA	0.223	0.255	0.362*	−0.410*	0.354*	−0.407**
Volume	−0.019	−0.202	−0.399**	0.078	−0.369*	–

Note:—Significant *P* values: * $P < .05$; ** $P < .01$; *** $P < .001$

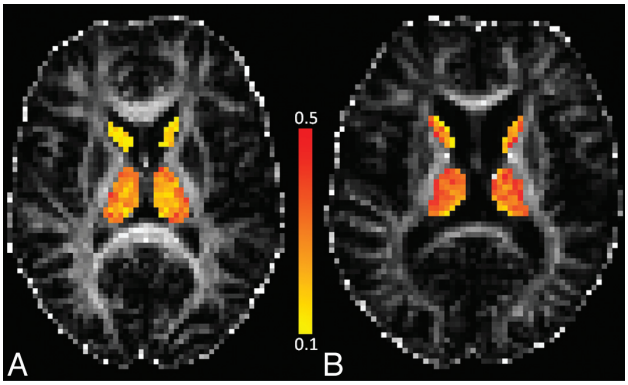

Fig 4. FA maps of a control subject (*A*) and a SP MS patient (*B*). The FA in the thalamus and caudate is color coded to highlight the heterogeneously pixelated appearance of the thalamus compared with the more homogeneous caudate nucleus. In the control subject, the FA (mean ± SD) was 0.156 ± 0.053 in the caudate and 0.267 ± 0.073 in the thalamus. In the patient with MS, these values were 0.236 ± 0.081 in the caudate and 0.303 ± 0.104 in the thalamus. While the mean FA is 66% higher in the patient's caudate compared with that of the control subject, this difference is only 13% in the thalamus. In contrast, the SD is of comparable magnitude for the patient and the control subject in the caudate, but shows an increase of 26% in the thalamus. This is consistent with reduced FA in damaged WM fibers in the thalamus and elevated FA in its subnuclei.

anisotropic organization.[27-29] Even though the FA changes in the thalamus are less marked than in the caudate, they are not inconsistent with our interpretation. We speculate that concurrent demyelination of intra-thalamic fibers could induce a FA decrease that will mitigate the proposed FA-elevating effect of dendritic dearborization in the thalamic subnuclei. This explanation, however, remains speculative, because it is unclear that the FA behavior of macroscopic WM tracts, which can fill entire voxels, translates to behavior in areas where oriented myelinated fibers occupy only fractions of voxels and are admixed with GM.

Alternatively, other pathologic processes, including an increased intracellular pool of restricted water molecules associated with cell swelling, could explain an increase in FA. Further animal and human work, applying newer DTI methodology (eg, composite hindered and restricted model of diffusion, or CHARMED[30]) and different experimental designs (including longitudinal studies) will be required to shed light on the relative merits of the above interpretations. The inverse correlation observed between FA and volume in both caudate and thalamus further supports a potential role for FA as a marker of neurodegeneration and as a predictor of subsequent atrophy (Fig 3). In fact, macroscopic bulk tissue loss (ie, atrophy) most likely results from continued microscopic damage to brain parenchyma. Initially, brain bulk might remain unchanged despite microscopic damage, due to sufficient residual mechanical scaffolding of the brain. In addition to the intrinsic damages of the GM structures, these changes may also result from WM lesions occurring along afferent or efferent pathways, leading to antero- or retrograde neurodegeneration. Indeed, the correlation observed between FA, as well as volume, and T2-LL suggests that WM lesions could weaken axonal integrity and lead to progressive wallerian degeneration and neuronal damage in remote GM structures. However, longitudinal studies are needed to validate this hypothesis against the alternate possibility that WM and GM are concomitantly attacked by the inflammatory and degenerative processes underlying MS.

Volume measurements demonstrated significant atrophy of the thalamus during the RR phase of MS, while caudate atrophy was statistically significant only in the more advanced SP phase of the disease (Table 2). In RR patients, reduced thalamic volume is accompanied by a moderate increase in FA, while a more marked increase in FA was observed in the caudate nuclei, despite no significant change in mean volumes. The relative difference in FA between RR patients and controls is 2.5 times as large in the caudate compared with the thalamus (0.235/0.195 = 20.5% versus 0.325/0.301 = 8.0%; Table 2). In SP patients, both structures were more severely atrophied, and their mean FA increased even further. The relative difference in FA between SP and RR patients is 3 times as large in the caudate compared with the thalamus (0.270/0.235 = 14.9% versus 0.341/0.325 = 4.9%; Table 2). These results suggest that FA is more sensitive to pathologic GM changes than gross volumetric measurement. Furthermore, reduced thalamic volume, presumably resulting from concomitant GM and WM damage, is not accompanied by the same degree of net FA change, because FA decreases in WM may be attenuated by concomitant FA increases in GM subnuclei. Taken together, our findings suggest that, in addition to the postulated damage to neuronal bodies and dendrites, the thalami are also affected by direct demyelination of the local WM fibers, in agreement with histopathologic studies.[31] Caudate and thalamic nuclei play a major role in executive functioning. Damage to these structures might be responsible for a range of motor, cognitive, and sensory disabilities. This is consistent with the significant correlation that we found between the FA of thalamus and caudate with EDSS and MSFC scores (Table 3), even though our experimental design is inadequate to determine causal relationships between specific structural alterations and functional deficits.

This study suffers from several methodologic limitations. First, the relatively low spatial resolution (due in part to the use of 1.5T MR imaging as opposed to 3T, as used in previous studies[15,16]) and the geometric distortions of DTI data due to EPI acquisition can impair the ROI registration with high-resolution anatomic images. Second, automatic segmentation can entail substantial partial volume effects by including tissue compartments adjacent to the structures of interest, such as isotropic CSF (FA $<$ 0.07) or highly anisotropic WM (FA $>$ 0.4). To limit these potential biases, a 1-voxel erosion was applied to the ROIs to reduce the partial volume effect at tissue boundaries, and the ROI position was checked for misalignment by an experienced rater. These methodologic biases were more evident in the results of automated overlay segmentation compared with the results of direct manual outlining, which tended to identify smaller ROIs (data not shown). Third, FA measurement in tissues with low anisotropy remains challenging.[32-34] In GM, the first 2 eigenvalues—λ1 and λ2—are of similar magnitude, and cannot be ranked and sorted with sufficient confidence.[32] We therefore reported only the rotationally invariant FA and MD parameters. To estimate the contribution of noise, we measured the FA in the CSF (FA_{CSF} = 0.044 ± 0.005) and found that it may represent a bias of 16%–19% in the caudate and 12%–14% in the thalamus of RR and SP patients, respectively. However, it remains unclear whether the noise measured in the CSF is the same as that present in measurements of other tissues with different diffusivity characteristics, such as GM or WM. Therefore, there remains a possibility that group differences may be driven by differences in the behavior of noise. Notwithstanding the aforementioned potential limitation, our scan–rescan reproducibility measurements showed a variation coefficient for FA of 2.6% in the thalamus and 4.7% in the caudate, supporting the reliability of our findings and the potential applicability of this measure to future longitudinal studies.

Conclusions

We believe that increased FA in the caudate and thalamus reflects progressive GM degeneration in patients with RR and SP MS. This measure may constitute a sensitive marker of MS pathologic processes, such as loss of dendrites and/or swelling of neuronal cell bodies.

Acknowledgments

The authors would like to express their gratitude to the staff of "CERMEP-Imagerie du Vivant" for their assistance in the acquisition of the data.

Disclosures: Charles Guttmann—*UNRELATED: Consultancy:* Tibotec Therapeutics, Johnson & Johnson, Comments: One-time ad hoc advisory consultant; *Grants/Grants Pending:* Teva Neuroscience;* *Stock/Stock Options:* Novartis, Roche, GSK, Pfizer, Nestle, Alnylam, Comments: Stockholder. (**Money paid to institution.*)

References

1. Charcot J. **Histologie de la sclérose en plaques** [in French]. *Gas Hop (Paris)* 1868;141:554–58
2. Dawson JW. **The histology of multiple sclerosis.** *Trans R Soc (Edinb)* 1916;50:517–740
3. Brownell B, Hughes JT. **The distribution of plaques in the cerebrum in multiple sclerosis.** *J Neurol Neurosurg Psychiatry* 1962;25:315–20
4. Kidd D, Barkoff F, McConnell R, et al. **Cortical lesions in multiple sclerosis.** *Brain* 1999;122(Pt1):17–26
5. Miller DH, Barkhof F, Frank JA, et al. **Measurement of atrophy in multiple sclerosis; pathological basis, methodological aspects and clinical relevance.** *Brain* 2002;125:1676–95
6. Zivadinov R, Cox JL. **Neuroimaging in multiple sclerosis.** *Int Rev Neurobiol* 2007;79:449–74
7. Mesaros S, Rocca MA, Absinta M, et al. **Evidence of thalamic grey matter loss in pediatric multiple sclerosis.** *Neurology* 2008;70:1107–12
8. Tao G, Datta S, He R, et al. **Deep grey matter atrophy in multiple sclerosis: A tensor based morphometry.** *J Neurol Sci* 2009;282:39–46
9. Sepulcre J, Sastre-Garriga J, Cercignani M, et al. **Regional grey matter atrophy in early primary progressive multiple sclerosis: a voxel-based morphometry study.** *Arch Neurol* 2006;63:1175–80
10. Audoin B, Davies GR, Finisku L, et al. **Localization of grey matter atrophy in early RRMS: a longitudinal study.** *J Neurol* 2006;253:1495–501
11. Bermel RA, Bakshi R. **The measurement and clinical relevance of brain atrophy in multiple sclerosis.** *Lancet Neurol* 2006;5:158–70
12. Khaleeli Z, Cercignani M, Audoin B, et al. **Localized grey matter damage in early primary progressive multiple sclerosis contributes to disability.** *Neuroimage* 2007;37:253–61
13. Rovaris M, Gass A, Bammer R, et al. **Diffusion MRI in multiple sclerosis.** *Neurology* 2005;65:1526–32
14. Ge Y, Law M, Grossman RI. **Applications of diffusion tensor MR imaging in multiple sclerosis.** *Ann N Y Acad Sci* 2005;1064:202–19
15. Hasan KM, Halphen C, Kamali A, et al. **Caudate nuclei volume, diffusion tensor metrics, and T(2) relaxation in healthy adults and relapsing-remitting multiple sclerosis patients: implications for understanding grey matter degeneration.** *J Magn Reson Imaging* 2009;29:70–77
16. Tovar-Moll F, Evangelou IE, Chiu AW, et al. **Thalamic involvement and its impact on clinical disability in patients with multiple sclerosis: a diffusion tensor imaging study at 3T.** *AJNR Am J Neuroradiol* 2009;30:1380–86
17. McDonald WI, Compston A, Edan G, et al. **Recommended diagnostic criteria for multiple sclerosis: guidelines from the International Panel on the Diagnosis of Multiple Sclerosis.** *Ann Neurol* 2001;50:121–27
18. Fischl B, Salat DH, Busa E, et al. **Whole brain segmentation: automated labeling of neuroanatomical structures in the human brain.** *Neuron* 2002;33:341–55
19. Fischl B, Salat DH, van der Kouwe AJ, et al. **Sequence-independent segmentation of magnetic resonance images.** *Neuroimage* 2004;23:S69–84
20. Smith SM, Jenkinson M, Woolrich MW, et al. **Advances in functional and structural MR image analysis and implementation as FSL.** *NeuroImage* 2004;23:208–19
21. Smith SM. **Fast robust automated brain extraction.** *Hum Brain Mapp* 2002;17:143–55
22. Souplet JC. *Évaluation de l'atrophie et de la charge lésionnelle sur des séquences IRM de patients atteints de sclérose en plaques* [in French]. PhD thesis, Université de Nice Sophia-Antipolis 2009
23. Hasan KM, Halphen C, Boska MD, et al. **Diffusion tensor metrics, T2 relaxation, and volumetry of the natural aging human caudate nuclei in healthy young and middle-aged adults: possible implications for the neurobiology of human brain aging and disease.** *Magn Reson Med* 2008;59:7–13
24. Hasbani MJ, Schlief ML, Fisher DA, et al. **Dendritic spines lost during glutamate receptor activation reemerge at original sites of synaptic contact.** *J Neurosci* 2001;21:2393–403
25. Trapp BD, Wujek JR, Criste GA, et al. **Evidence for synaptic stripping by cortical microglia.** *Glia* 2007;55:360–68
26. Kim IJ, Beck HN, Lein PJ, et al. **Interferon gamma induces retrograde dendritic retraction and inhibits synapse formation.** *J Neurosci* 2002;22:4530–39
27. Mori S, Itoh R, Zhang J, et al. **Diffusion tensor imaging of the developing mouse brain.** *Magn Reson Med* 2001;46:18–23
28. Mukherjee P, Miller JH, Shimony JS, et al. **Diffusion-tensor MR imaging of gray and white matter development during normal human brain maturation.** *AJNR Am J Neuroradiol* 2002;23:1445–56
29. Zhang J, Richards LJ, Yarowsky P, et al. **Three-dimensional anatomical characterization of the developing mouse brain by diffusion tensor microimaging.** *Neuroimage* 2003;20:1639–48
30. Assaf Y, Basser PJ. **Composite hindered and restricted model of diffusion (CHARMED) MR imaging of the human brain.** *Neuroimage* 2005;27:48–58
31. Lumsden C. **The neuropathology of multiple sclerosis.** In: Vinken P, Bruyn G. *Handbook of Clinical Neurology. Volume 9. Multiple Sclerosis and Other Demyelinating Diseases.* New York: American Elsevier;1970:217–309
32. Wheeler-Kingshott C, Cercignani M. **About "axial" and "radial" diffusivities.** *Magn Reson Med* 2009;61:1255–60
33. Jones DK, Cercignani M. **Twenty-five pitfalls in the analysis of diffusion MRI data.** *NMR Biomed* 2010;23:803–20
34. Pierpaoli C, Basser PJ. **Toward a quantitative assessment of diffusion anisotropy.** *Magn Reson Med* 1996;36:893–906